Parasitology Research
https://doi.org/10.1007/s00436-022-07732-z

RESEARCH

Advancing understanding of the taxonomy and diversity of the genus *Contracaecum* in the great white pelican (*Pelecanus onocrotalus*)

Monica Caffara[1] · Perla Tedesco[1] · Nadav Davidovich[2] · Sean A. Locke[3] · Andrea Gustinelli[1] · Roni King[4] · Michelle Nuytten[1] · Marialuisa Nuzzo[1] · Maria Letizia Fioravanti[1]

Received: 10 June 2022 / Accepted: 12 November 2022

Abstract

Despite the wide distribution and health importance of anisakids of the genus *Contracaecum*, epidemiological data on their occurrence in definitive bird hosts are scarce, particularly from certain parts of the world that represent important wintering sites or migration stopovers for different bird species. In the present study, *Contracaecum* spp. infecting six great white pelicans (*Pelecanus onocrotalus*) in Israel were identified using light and scanning electron microscopy and phylogenetic analyses of nuclear internal transcribed spacer (ITS) and mitochondrial cytochrome *c* oxidase II (*cox*2). A PCR–RFLP method was also developed and applied to screen large numbers of *Contracaecum* parasites. Most (415/455) worms recovered were *C. micropapillatum*, followed by *C. gibsoni* (31/455), *C. quadripapillatum* (8/455), and *C. multipapillatum* E (1/455). *Contracaecum micropapillatum* from Israel and *C. bancrofti* from Australia are distinguishable by *cox*2 but less well resolved with ITS sequences, and could not be distinguished morphologically. Worms with *cox*2 matching *C. gibsoni* had ITS matching specimens identified as *C. multipapillatum* A. To the authors' knowledge, this represents the first of such studies in Israel and provides useful data on the ecology and distribution of different *Contracaecum* species of health and economic interest.

Keywords *Contracaecum* · Taxonomy · Great white pelican · Israel

Introduction

Anisakids of the genus *Contracaecum* Railliet and Henry 1912 are widely distributed in aquatic ecosystems (freshwater, brackish, and marine) where they undergo a heteroxenous life cycle, involving a wide range of paratenic hosts (crustaceans, planktivorous, and piscivorous fish; Anderson 2000; Valles-Vega et al. 2017) and definitive hosts, including marine mammals (pinnipeds, cetaceans) and piscivorous birds (Mattiucci and Nascetti 2008).

The genus *Contracaecum* comprises over 60 species, the majority of which have been described from fish-eating birds but also in marine mammals (Yamaguti 1935; Hartwich 1964; Baruš et al. 1978; Ángeles-Hernández et al. 2020). In birds, massive infections may occur as a result of the continuous ingestion of paratenic hosts; third-stage larvae undergo further development and moult, becoming fourth stage and eventually adults in the proventriculus and stomach (Fagerholm and Overstreet 2008), where they cause hemorrhages, ulcerations, and necrosis, leading in some instances to a fatal outcome (Rokicki et al. 2011; Kumar et al. 2019).

The taxonomic status of several *Contracaecum* spp. is uncertain due to their morphological similarity and needs to be investigated with both morphological and molecular analysis. One pair of species needing such attention is *Contracaecum bancrofti* and *C. micropapillatum*. Johnston and Mawson (1941) described *Contracaecum bancrofti* from the Australian pelican *Pelecanus conspicillatus* sampled throughout Eastern Australia. The adults of *C. bancrofti*

Section Editor: Shokoofeh Shamsi

Monica Caffara and Perla Tedesco contributed equally.

✉ Monica Caffara
monica.caffara@unibo.it

[1] Department of Veterinary Medical Sciences, Alma Mater Studiorum University of Bologna, Via Tolara Di Sopra 50, 40064 Ozzano Emilia (BO), Italy

[2] Israeli Veterinary Services, 5025001 Bet Dagan, Israel

[3] Department of Biology, University of Puerto Rico, Box 9000, Mayagüez 00681-9000, Puerto Rico

[4] Israel Nature and Parks Authority, 3 Am Ve'Olamo St, 95463 Jerusalem, Israel

Published online: 25 November 2022

were distinguished from an older, similar species described in Croatia, *C. micropapillatum* (Stossich 1890), on the basis of the position of vulva and size of eggs in females, and on the length of spicules in males (Johnston and Mawson 1941). However, Hartwich (1964) considered *C. bancrofti* a synonym of *C. micropapillatum*. Based on a variety of morphometric data, Shamsi et al. (2009) considered *C. bancrofti* to be valid and provided the first ITS rDNA sequences from this species. Although aware of the work of Shamsi et al. (2009), Li et al. (2016) nonetheless considered the two species as synonyms and reported *C. micropapillatum* in North America, Africa, Europe, China, and Australia, albeit without providing any support for this decision.

Adults of *C. bancrofti* infecting *Pelecanus conspicillatus* have been reported from several parts of Australia, including Peron Island in the Northern Territory, Thompson River and Burnett River in Queensland, Sydney Zoological Gardens in New South Wales, Geelong and Healesville in Victoria, and Morgan in South Australia (Johnston and Mawson 1941; Shamsi et al. 2009). Although Shamsi et al. (2009) considered *C. bancrofti* endemic in Australia, this species has also been reported in the American white pelican *P. erythrorhynchos* along the coasts of Texas (McDaniel and Patterson 1966) and in Mexico (Yamaguti 1961). To our knowledge, neither the occurrence of *C. bancrofti* outside Australia nor its genetic differentiation from *C. micropapillatum* has been assessed with molecular data. This is partly because different genetic markers have been sequenced in these two species, namely ITS rDNA in *C. bancrofti* (Shamsi et al. 2009), 28S rDNA and *cox*2 mtDNA in *C. micropapillatum* (Nadler and Hudspeth 2000; Mattiucci et al. 2008, 2010).

The ITS rDNA sequences from adult *C. bancrofti* (Shamsi et al. 2009) allowed identification of larval stages in freshwater fishes, including *Cyprinus carpio* (Shamsi et al. 2018a), *Carassius auratus*, *Gambusia holbrooki*, *Hypseleotris* sp., *Melanotaenia fluviatilis*, *Misgurnus anguillicaudatus*, *Nematalosa erebi*, and *Retropinna semoni* in eastern Australia (Shamsi et al. 2018b). Possibly due to their small size, location deeply embedded in fish host tissues, and paucity of morphological features useful for species identification, the larvae of *C. bancrofti* have not been reported elsewhere. Nevertheless, the diversity of infected hosts (eight fish species from eight different families) suggests that *C. bancrofti* may also occur in a variety of other host species.

The present study is part of a larger project focused on the parasitic fauna of piscivorous birds collected in Israel. Sampled birds included Pelecanidae belonging to the species *P. onocrotalus*, which were found infected with parasitic nematodes of the genus *Contracaecum*. The aim of this work was to characterize these parasites to the species level with morphometrical (by both light microscopy and scanning electron microscopy—SEM) and molecular methods based on two markers (i.e., ITS rDNA and *cox*2 mtDNA) to confirm their taxonomic position. To date, no such studies have been carried out in Israel, and therefore our work was also intended to elucidate the ecology and distribution of *Contracaecum* species in scarcely investigated hosts and geographical areas.

Materials and methods

Contracaecum sampling

Four hundred and fifty-five adults of *Contracaecum* spp. were collected from the gastric mucosa of six great white pelican (*Pelecanus onocrotalus*) collected and processed fresh, from five localities under permits 2020/42659 and 2021/42855 from the Israel Nature and Parks Authority (Fig. 1). The nematodes were washed in saline and preserved in 70% ethanol for morphological and molecular analysis. For some adults, the anterior and posterior portions were preserved in 10% neutral buffered formalin for SEM. Moreover, two additional specimens of *Contracaecum bancrofti* were obtained from *Pelecanus conspicillatus* sampled in Australia.

Morphological study

Fifty males and 50 females were randomly selected from the 6 Israeli birds and observed under a dissection microscope to first evaluate gross morphology and to record total length (TL), then under a light microscope (Leica Microsystems, Wetzlar, Germany) with the aid of a digital Nikon DS-Fi1 camera and image-acquisition software (Nikon Nis-Elements D3.0). A section of each worm was then removed for DNA extraction (central 5 mm, where taxonomically informative features are absent). Anterior and posterior portions of the parasite body then were clarified in Amman's lactophenol to measure internal structures by light microscope. Morphometric analysis was conducted following Yamaguti (1935), Hartwich (1964), and Baruš et al. (1978). Measurements are given in millimeters unless otherwise indicated. The two specimens of *C. bancrofti* from Australia were subject to the same treatment.

For SEM, anterior and posterior portions of the nematodes were dehydrated through a graded ethanol series, subjected to critical point drying, sputter-coated with gold palladium, and observed using a Phenom XL G2 Desktop SEM (Thermo Fisher Scientific, Eindhoven, The Netherlands) operating at 5 kV.

Measurements of specimens of *C. micropapillatum* and *C. bancrofti* were compared using data from the present and other studies using non-metric multidimensional scaling and ANalysis Of SIMilarity (ANOSIM) (999 permutations,

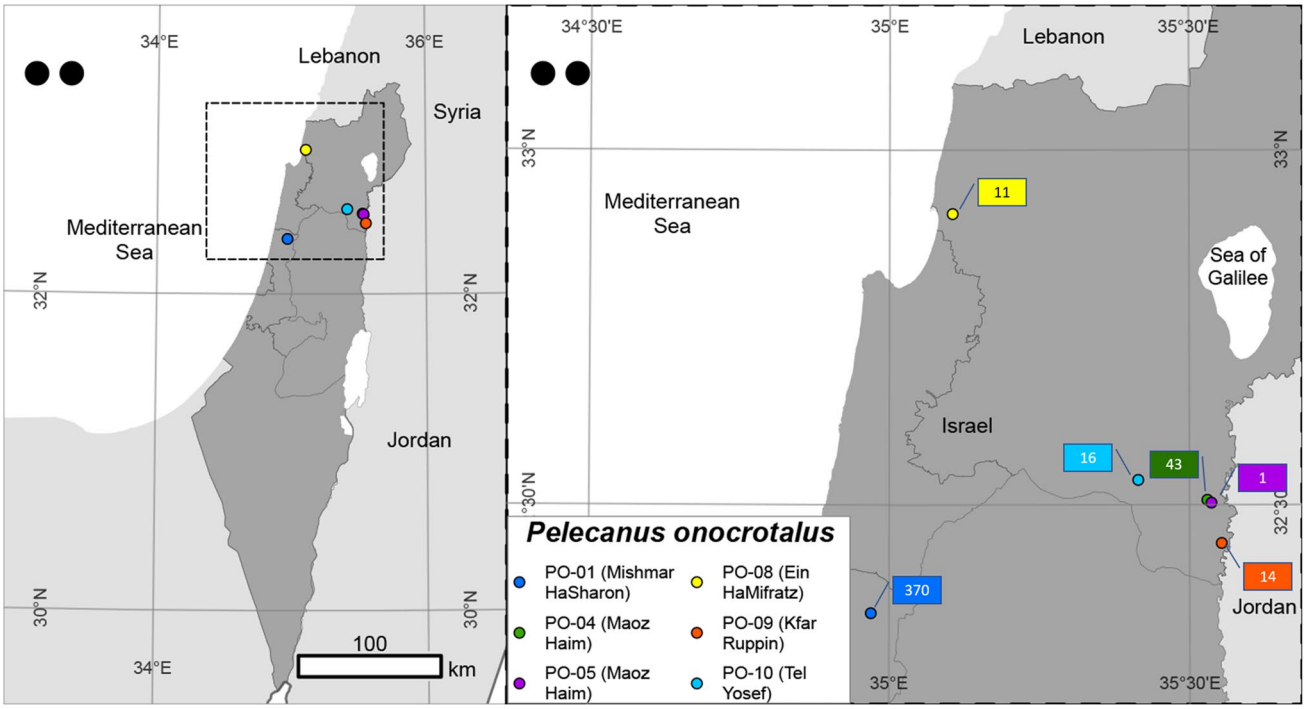

Fig. 1 Map of Israel with detail of the sampling locality together with the number of *Contracaecum* spp. collected from each *Pelecanus onocrotalus*

crossed design of species × worm sex) in PRIMER-E (Auckland, NZ). Morphometric distances were based on normalized measurements of eight features (lengths of whole body, esophagus, intestinal cecum, ventricular appendix, tail, left and right spicules, and distance of vulva to anterior end, transformed by subtracting the mean from the observed value and dividing the result by the standard deviation, for each variable). As only two specimens of *C. bancrofti* were available, and individual-specimen-level data from *C. micropapillatum* are not available from prior publications, six additional data points (equivalent to artificial specimens) were extracted from other studies based on reported minimum, maximum, and mean (if given) or range midpoint, for each sex, for each of the eight aforementioned measurements.

Molecular study

For molecular analysis, genomic DNA was initially extracted from 51 adults using a PureLink® Genomic DNA Kit (Life Technologies, Carlsbad, CA, USA) following the manufacturer's instructions. The ITS rDNA was amplified with primers NC5_f (5′-GTAGGTGAACCTGCGGAAGGATCATT-3′) and NC2_r (5′-TTAGTTTCTTCCTCCGCT-3′) (Zhu et al. 1998). A fragment of *cox*2 mtDNA was amplified from 33 adults (among the 51) with primers 211_f (5′-TTTTCTAGT TATATAGATTGRTTTYAT-3′) and 210_r (5′-CACCAACTC TTAAAATTATC-3′) of Mattiucci et al. (2008) following the same protocol. The PCR products were electrophoresed on a 1% agarose gel stained with SYBR Safe DNA Gel Stain (Thermo Fisher Scientific, Carlsbad, CA, USA) in 0.5X TBE. For sequencing, the amplicons were excised and purified by Nucleo-Spin Gel and PCR Clean-up (Mackerey-Nagel, Düren, Germany), and sequenced with an ABI 3730 DNA analyzer (StarSEQ, Mainz, Germany). The DNA trace files were assembled with Contig Express (VectorNTI Advance 11 software, Invitrogen, Carlsbad, CA, USA), and the consensus sequences of the ITS rDNA after separating the two regions (ITS1 and ITS2) and *cox*2 mtDNA were compared with published data by BLAST tools (https://blast.ncbi.nlm.nih.gov/Blast.cgi). Multiple sequence alignments were performed using BioEdit 7.2.5 (Hall 1999); p-distance and maximum-likelihood (ML) tree (T92 + G + I substitution model for ITS and KHY + G + I for *cox*2, bootstrap of 1000 replicates for both genes) were obtained using MEGA 7 (Kumar et al. 2016). The ITS1 and ITS2 rDNA sequences were concatenated and used to build a ML tree together with the sequences of *Contracaecum* spp. reported by Mattiucci et al. (2020). The *cox*2 gene was also aligned with the sequences reported by Mattiucci et al. (2020), with *Pseudoterranova ceticola* (DQ116435) and *Anisakis pegreffii* (MT912471) as outgroups. The sequences generated in this study have been deposited in GenBank under accession numbers ON714944-88 (cox2 mtDNA) and ON736806-38 (ITS rDNA).

The initial sequencing of *Contracaecum* from Israel indicated mixed species infections in individual birds; molecular work was conducted on all remaining adult worms. The middle portions of 404 adult males and females were subjected to a fast DNA extraction method using Chelex®100 (Sigma-Aldrich, Darmstadt, Germany). Briefly, 300 µl of 5% Chelex®100 solution in sterile DNA/RNA free molecular grade water was added to the central piece of body and heated at 95 °C for 10 min. and then centrifuged at full speed for 5 min. The supernatant was removed and diluted 1:10 for downstream molecular analyses. The ITS rDNA of the extracts was amplified as reported above, and then 10 µl was subjected to PCR–RFLP with the restriction enzymes *Msp*I (Zhu et al. 2007) and *Ssp*I to distinguish among species of *Contracaecum*. The second enzyme was selected after running an in-silico digestion of the whole ITS rDNA of some sequenced specimens, with the software NEBcutter 3.0 (https://nc3.neb.com/NEBcutter/). After digestion (37 °C for 90 min), the specimens were electrophoresed on a 2% agarose gel stained with SYBR Safe DNA Gel Stain (Thermo Fisher Scientific, Carlsbad, CA, USA) in 0.5X TBE for 90 min. In each digestion reaction, previously Sanger-sequenced specimens were included as positive controls.

Results

Molecular analyses

Overall, of 455 adult worms from six Israeli pelicans examined with a combination of morphometric and molecular analyses, 415 were identified as *C. micropapillatum*, 31 as *C. gibsoni*, 8 as *C. quadripapillatum*, and 1 as *C. multipapillatum* E (Table 1). As described below, most of these identifications were based on PCR–RFLP, and the entire ITS rDNA array was sequenced in 51 worms from Israel, with partial *cox*2 sequenced in 33 of the same specimens. Both ITS rDNA and *cox*2 mtDNA were also sequenced in two specimens of *C. bancrofti* from *P. conspicillatus* in Australia, and these data supported the distinct status of *C. bancrofti*.

Thirty-four worms from Israel with identical ITS rDNA sequences were 99.5% similar to adults of *C. bancrofti* from Australia, comprising data from Shamsi et al. 2009 (EU839568-EU839566) and from two specimens of *C. bancrofti* from Australia newly sequenced in the present study. In phylogenetic analysis, all the aforementioned ITS sequences fell in a well-supported clade containing two subclades of sequences from Israel and Australia with moderate support (95%, 79%) (Fig. 2). Sequences of *cox*2 from 25 of these 34 adult worms from Israel matched (97–99.2% similarity) those of *C. micropapillatum* (EU852350, Mattiucci et al. 2010, EF513514-16 and EF122206-07, Mattiucci et al. 2008) and were 92.6% similar to the *cox*2 from two specimens of *C. bancrofti* from Australia, newly sequenced herein. In phylogenetic analysis of *cox*2, specimens from Israel and Australia were resolved into two clades with strong (≥98%) bootstrap support (Fig. 3). Taken together, these analyses support the separation of *C. micropapillatum* and *C. bancrofti*. Further evidence of the validity of *C. bancrofti* occurred in the form of gaps in the ITS rDNA alignment. A 12-bp gap unique to *C. bancrofti* began at position 120 in ITS1, which corresponded to an insertion of "TTGCTAAATTAA" in *C. multipapillatum* sequences and "TTGCTTATTTAG" in *C. quadripapillatum*. At the 3′ end of ITS1, an insertion of 7 bp (position 420–426 bp, "TATTTAG") occurred in *C. bancrofti* only. In ITS2, we observed 3 insertions in the *C. bancrofti* sequences (position 449–456 bp "GAATATCT," position 495–507 bp "AAA GACGAGAAAA," and position 555–569 bp "TCCTTG CTTAGTTTG") corresponding to deletions in the other two species. The ITS sequences from the adult specimens of *C. micropapillatum* from Israel were also 99.7% similar to ITS from larvae of an unidentified species of *Contracaecum* from *Tilapia zillii* from Kenya (KF990496, Otachi et al. 2014), indicating a possible transmission path of this *C. micropapillatum*. The 34 ITS sequences of *C. micropapillatum* from Israeli pelicans differed by 2.5% from *C. multipapillatum* and 2.4–2.5% from *C. quadripapillatum*.

The ITS sequences of eight adults from Israel were 99.7% similar to *C. quadripapillatum* (OK138879-80, Hamouda and Younis 2022) from *Heterobranchus bidorsalis* from

Table 1 Details of the species of *Contracaecum* identified in each sampling locality (see Fig. 1). PO = *Pelecanus onocrotalus*

ID	Sampling locality	n. examined	*C. micropapillatum*	*C. gibsoni*	*C. quadripapillatum*	*C. multipapillatum* E
PO-01	Mishmar HaSharon	370	349	20	1	-
PO-04	Maoz Haim	43	31	11	1	-
PO-05	Maoz Haim	1	-	-	1	-
PO-08	Ein HaMifratz	11	11	-	-	-
PO-09	Kfar Ruppin	14	10	-	4	-
PO-10	Tel Yosef	16	14	-	1	1

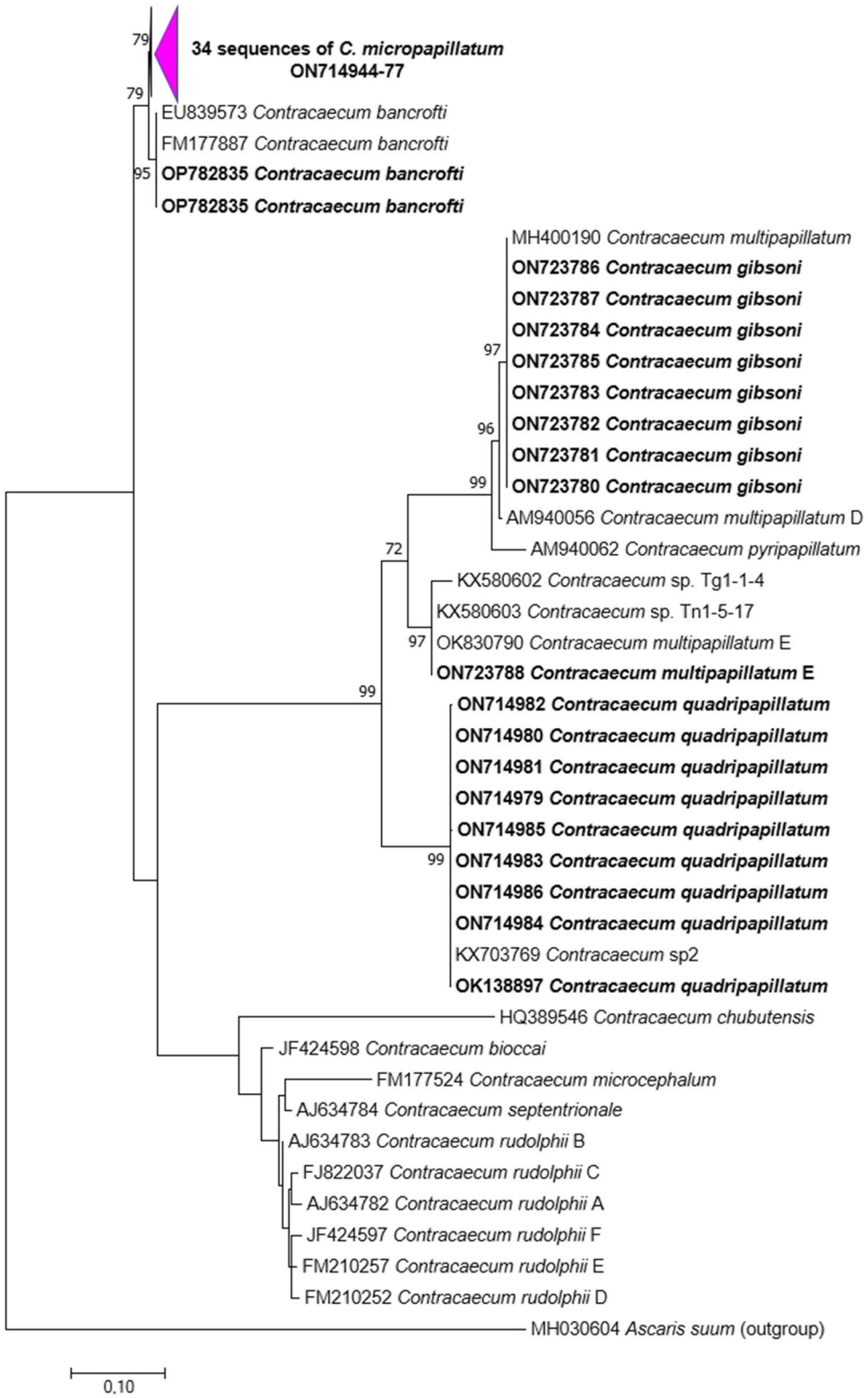

Fig. 2 Maximum-likelihood tree based on the concatenated ITS1-ITS2 rDNA sequences showing the relationship between *C. micropapillatum* (condensed, containing 34 sequences GB acc. n. ON714944-77), *C. bancrofti*, *C. gibsoni*, *C. quadripapillatum*, and *C. multipapillatum* E described in the present study (in bold) and the congeneric *Contracaecum* species. The tree is drawn to scale, with branch length measured in the number of substitutions per site

Lake Nasser (Egypt), identical to *Contracaecum* sp. 2 (MT477131) from an unknown fish species sampled in Ethiopia, 99.6% similar to *Contracaecum* sp. (MZ727197, Thabit and Abdallah 2022, unpublished) from *Lates niloticus* both from Egypt, and 99.3% similar to *Contracaecum* sp. 1–8 (FM210434, Shamsi and Aghazadeh-Meshgi 2011) from barboid fish in Iran. These ITS sequences formed a distinct and well-supported lineage in phylogenetic analysis

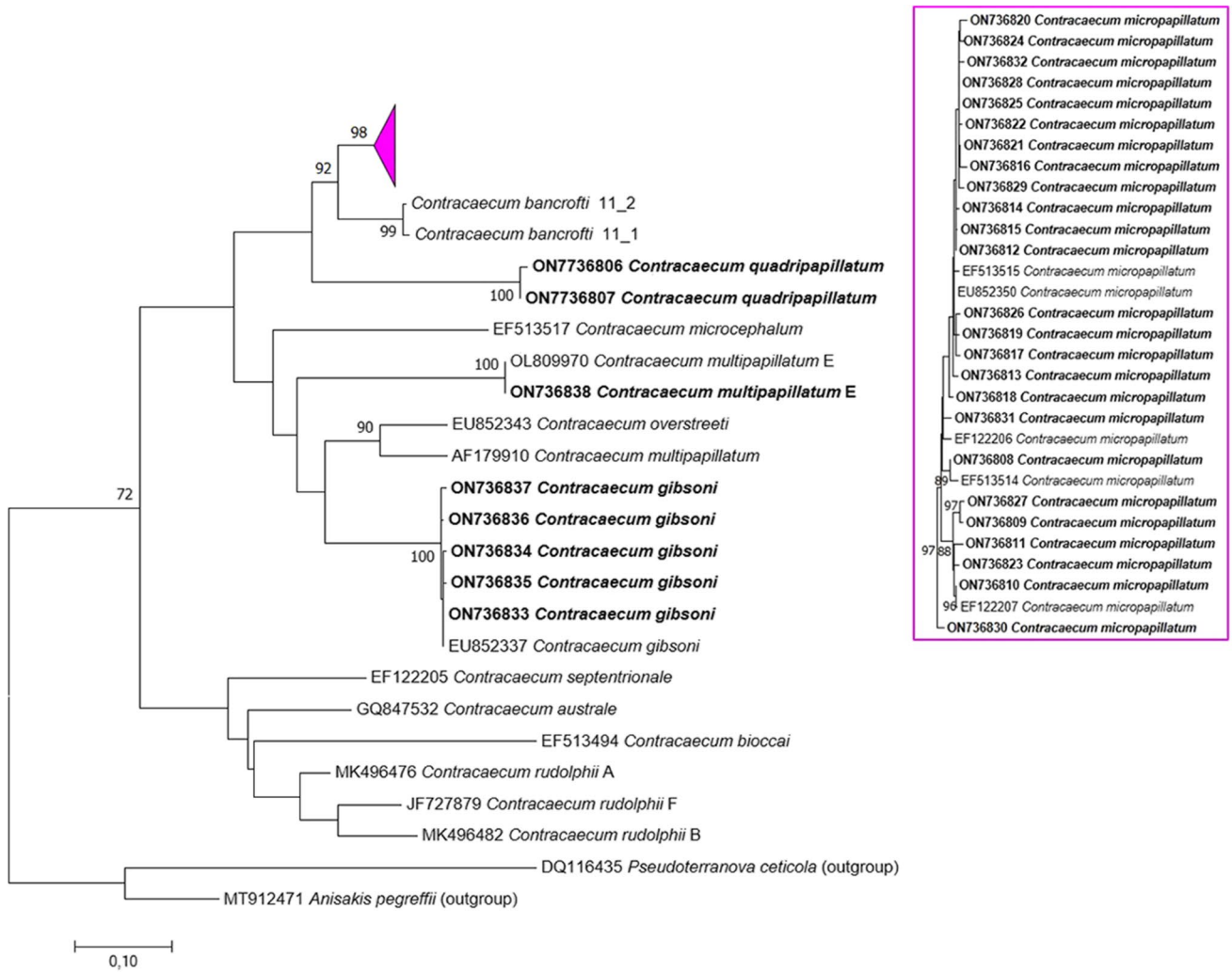

Fig. 3 Maximum-likelihood tree based on the *cox*2 mtDNA sequences showing the relationship between *C. micropapillatum* (condensed pink clade containing 25 sequences GB acc. n. ON736808-32, expanded at right), *C. bancrofti*, *C. gibsoni*, *C. quadripapillatum*, and *C. multipapillatum* E described in the present study (in bold) and other *Contracaecum* species. The inset at right shows sequences from the present study nested with *C. micropapillatum* of Mattiucci et al. (2008, 2010) from *P. onocrotalus* sampled in Egypt and Greece. The tree is drawn to scale, with branch length measured in the number of substitutions per site

(Fig. 2). The *cox*2 sequences of two the eight specimens in this clade were most similar (87.6%) to *C. osculatum* A sensu Nascetti et al. (JN786334). As described below, these worms were identified as *C. quadripapillatum*.

Another eight specimens yielded ITS sequences identical to *C. multipapillatum* (MH400190, Pronkina and Spiridonov 2018) from *Chelon auratus* from the Black Sea and with 98.7% similarity to *C. multipapillatum* D (AM940056, Shamsi et al. 2008) from Australian *P. conspicillatus*. In five of these eight adults with these ITS rDNA matching *C. multipapillatum*, *cox*2 showed 99.6–100% similarity with *C. gibsoni* (EU852337, syn *C. multipapillatum* A, Mattiucci et al. 2010) from *P. crispus* from Greece (intraspecific p-distance 0–0.1%).

In one adult specimen from Israel, both ITS (ON723788) and *cox2* (ON736838) were identical to *C. multipapillatum* E (OL830790, OL809970, Davidovich et al. 2022) from hybrid tilapia farmed in Israel.

Through PCR–RFLP analysis, 413 adults were identified as *C. micropapillatum*, 31 as *C. gibsoni*, 8 as *C. quadripapillatum*, and one as *C. multipapillatum* E. These results were based on *Msp*I banding patterns of 330–315–230 bp for *C. micropapillatum*, 560–360 bp for *C. gibsoni*, and 600–360 bp for *C. quadripapillatum*, while *C. multipapillatum* E was not digested. The enzyme *Ssp*I was able to distinguish better between *C. gibsoni* and *C. quadripapillatum*, producing 550–300 bp fragments for the former and no cut for the latter (undigested band of 1000 bp) (Fig. 4).

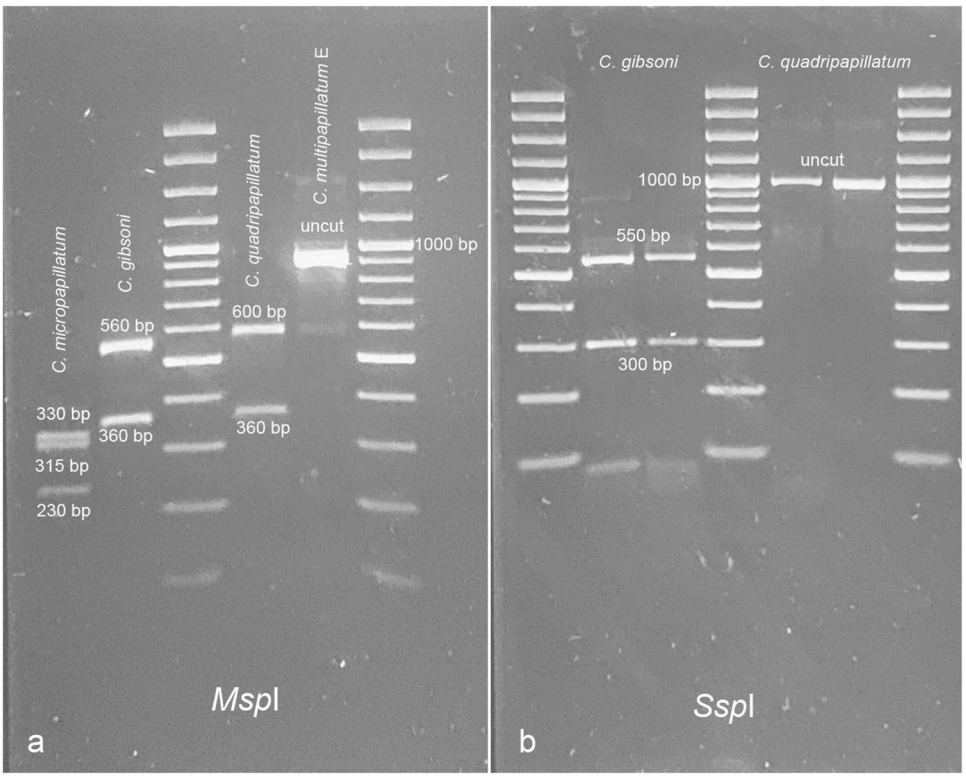

Fig. 4 PCR–RFLP pattern of *C. micropapillatum, C. gibsoni*, *C. quadripapillatum*, and *C. multipapillatum* E after digestion with *Msp*I (**a**) and *Ssp*I (**b**)

Morphological descriptions

Contracaecum micropapillatum Johnston and Mawson 1941

Synonym: *Ascaris micropapillata* Stossich 1890

Site in host: stomach.

Representative DNA sequences: ON714944-77 (ITS rDNA), ON736808-32 (*cox*2 mtDNA).

Adult stage: Body stout. Cuticle transversally striated. Lips longer than wide, one dorsal and two sub-ventral (Figs. 5a–b and 6a). Two oval cephalic papillae on dorsal lip and a single papilla on each subventral lip. Interlabium reaching approximately ¾ of lip length, narrow, wider at base, with distinctly bifurcated tip (Fig. 5c). Excretory pore at base of lips. Collar area with fine cuticular annulations interrupted laterally. Deirids at approximately same level as nerve ring. Esophagus muscular, ending in round ventriculus with short ventricular appendix. Intestinal caecum two to three times longer than ventricular appendix.

Males ($n=50$): Total length 10–34.2 (17.2 ± 4.9). Nerve ring 0.17–0.67 (0.48 ± 0.1) from anterior end. Esophagus 2.01–4.56 (3.27 ± 0.59) long, 12.3–25.5% (19.7%) of body length. Ventricular appendix 0.47–1.15 (0.85 ± 0.14) long, 17.8–42.1% (26.7%) of esophageal length. Intestinal cecum 1.47–3.79 (2.5 ± 0.5) long, 55.7–86.3% (75.8%) of esophageal length. Three pairs of double post-cloacal papillae (Fig. 5d). Phasmids approximately at level of third pair of post-cloacal papillae. Precloacal papillae simple, arranged in two longitudinal rows (Fig. 5e). Spicules similar, subequal, 8.6–19% (14%) of body length. Right spicule 1.02–3.37 (2.45 ± 0.56) long; left spicule 1.05–3.48 (2.4 ± 0.56) long, with rounded tip and folded longitudinal alae (Fig. 5f–g).

Females ($n=50$): Total length 10–40.7 (18.8 ± 9.4). Nerve ring 0.25–0.92 (0.45 ± 0.13) from anterior end. Esophagus 1.67–5.69 (3.29 ± 1.02) long, 12.7–22.3% (18.7%) of body length. Ventricular appendix 0.44–1.67 (0.81 ± 0.27) long and 14.2–40.2% (25.2%) of esophageal length. Intestinal cecum 1.34–4.87 (2.48 ± 0.84) long, 62.7–89.1% (75.6%) of esophageal length. Vulva in anterior half of body, 1.76–14.11 (6.68 ± 3.7) from anterior end (Fig. 6b); Tail conical, 0.17–0.54 (0.33 ± 0.09) long, with pointed tip (Fig. 6c–d).

Remarks

Overall, the validity of *C. bancrofti* was well supported by molecular data. While divergence levels and phylogenetic analysis of ITS did not present overwhelming support for considering Australian *C. bancrofti* separate from *C. micropapillatum* (the older species), the indels in the ITS alignment and all aspects of *cox*2 analysis provide strong support for both species. These results are not surprising, as ITS may vary little or not at all between recently separated species (Zhu et al. 2000; Blouin 2002).

Morphological analysis of genetically characterized specimens revealed no characters that clearly distinguish *C. bancrofti* and *C. micropapillatum*. As characterized by Johnston and Mawson (1941), *C. bancrofti* was reported having

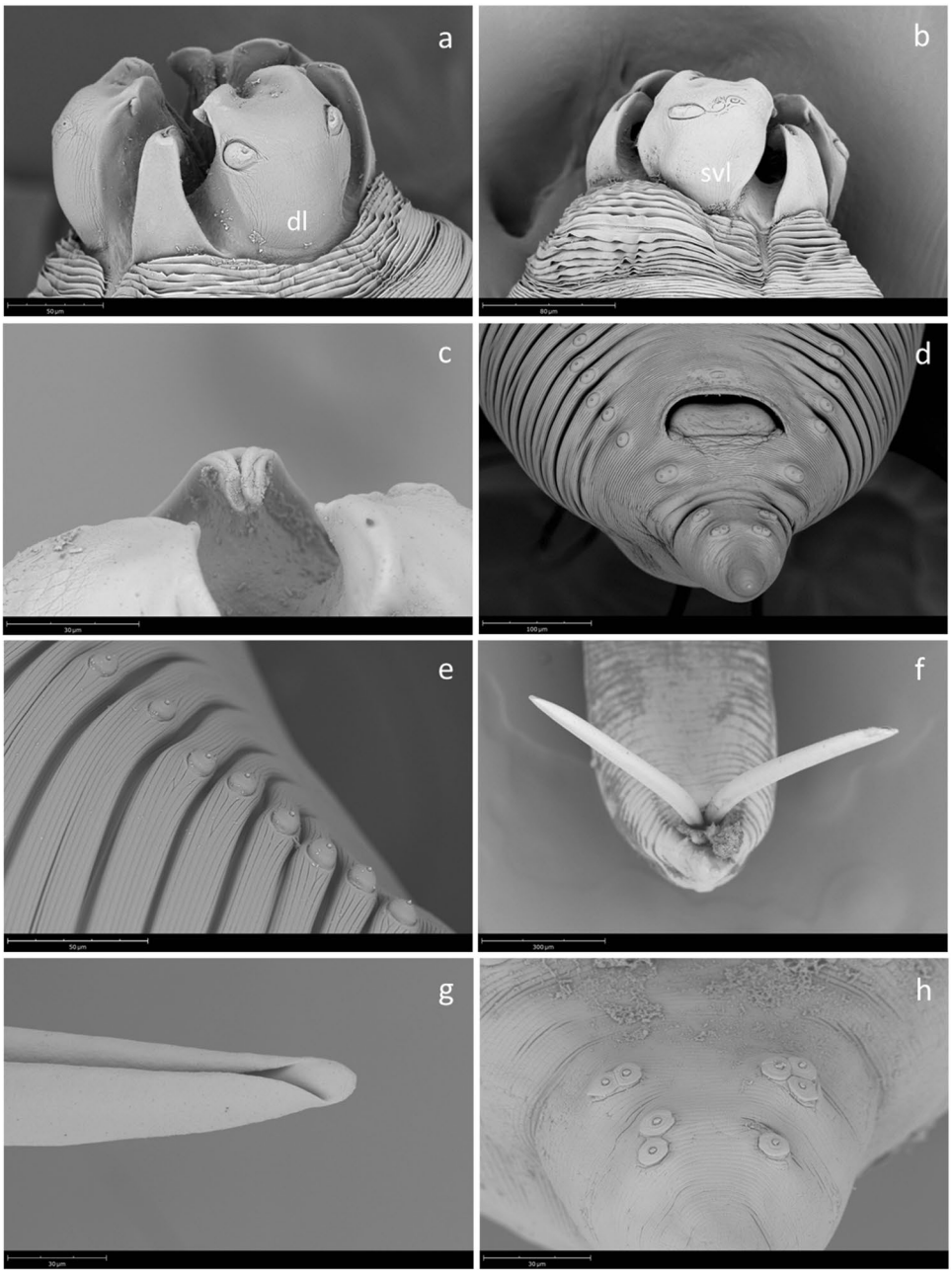

Fig. 5 SEM micrographs of *C. micropapillatum* adult males: **a**) anterior end, showing dorsal lip (dl); **b**) anterior end, showing subventral lip (svl); **c**) detail of bifid interlabium; **d**) ventral view of caudal end, showing two rows of single pre-cloacal papillae, and two rows of double post-cloacal papillae; **e**) detail of precloacal papillae; **f**) caudal end with everted spicule; **g**) detail of spicule tip; **h**) specimen with unusual pattern of post-cloacal papillae

interlabia with bifid tips and the male tail with three pairs of double papillae, and was differentiated from the morphologically similar *C. micropapillatum* based on the length of the spicules, size of the eggs, and position of the vulva.

Hartwich (1964), who considered *C. bancrofti* a synonym of *C. micropapillatum*, reported spicule lengths (1.21–3.53 mm) for *C. micropapillatum*, which closely overlap lengths we observed in 50 genetically identical specimens of this species (1.02–3.48 mm) collected in Israel. In contrast, spicules 2.2–2.8 mm long were measured by Johnston and Mawson (1941) in an unknown number of specimens of *C. micropapillatum*. In comparison, spicule lengths of 2.23–3.17 mm long were recorded in 18 specimens of *C. bancrofti* measured by Shamsi et al. (2009) and suggested that this narrower range of spicule lengths supported the validity of *C. bancrofti*, separate from *C. micropapillatum*, and raised the possibility that Hartwich's material included multiple species. Our results support the validity of *C. bancrofti*, as per Shamsi et al. (2009) but also indicate that spicule length variation may not be a useful character for distinguishing the two species.

The caudal papillae in the post-cloacal region also appear to be inconclusive for resolving *C. bancrofti* and *C. micropapillatum*, as these show the same pattern in both

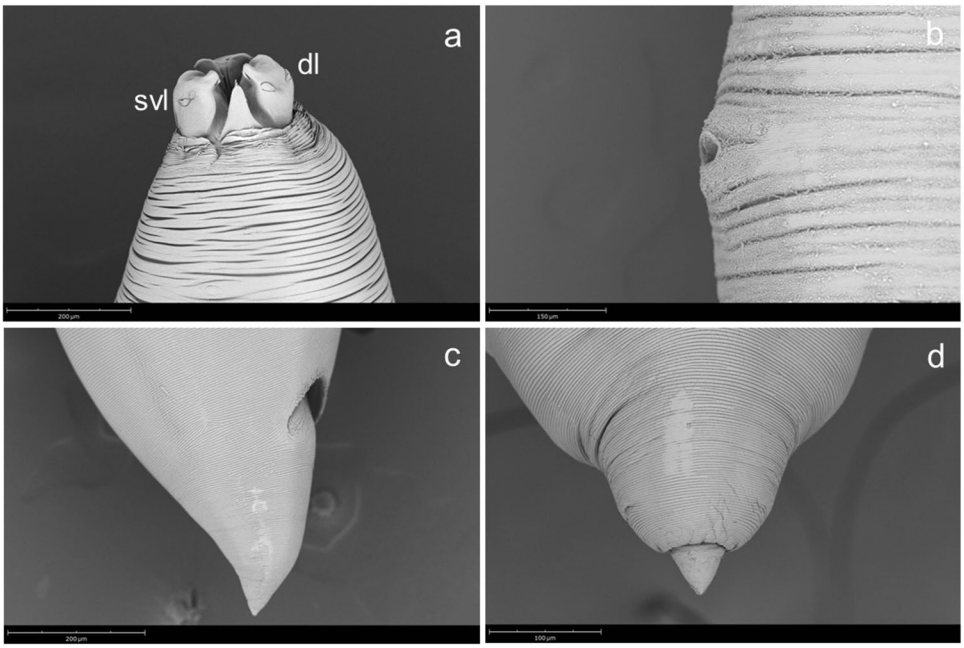

Fig. 6 SEM micrographs of *C. micropapillatum* adult females: **a**) anterior end, showing dorsal lip (dl) and subventral lip (svl); **b**) detail of vulva; **c**) lateral view of caudal end; **d**) detail of caudal tip

species, i.e. three pairs of double papillae (Stossich 1890; Cram 1927; Hartwich, 1964; Shamsi et al. 2009). The SEM micrographs of *C. micropapillatum* genetically characterized in the present study show the first pair of post-cloacal papillae are generally fused (Fig. 5d), while the second and third pairs may be single but adjacent, or shifted backwards (Fig. 5h), possibly due to differences in the developmental stage, or to intraspecific variability.

In genetically identified female specimens of *C. micropapillatum*, the distance of the vulva from anterior end varied from 1.8 to 14.1 mm, which overlaps data reported by Shamsi et al. (2019) and Hartwich (1964). Therefore, female morphology and morphometry are not of value in distinguishing *C. bancrofti* from *C. micropapillatum* and, in fact, have seldom been used in specific diagnosis of *Contracaecum* and other anisakids.

Other morphometric features of the adult stage (total body length, length of esophagus, intestinal cecum, ventricular appendix) of *C. micropapillatum* were on average higher in Stossich (1896) and Cram (1927) compared to data reported by Hartwich (1964). Our values include also measurements of smaller specimens and are more similar to the ranges reported by Hartwich (1964).

Additionally, both *C. micropapillatum* (Stossich 1890; Hartwich 1964 as reported in Baruš et al. 1978) and *C. bancrofti* (Johnston and Mawson 1941; Shamsi et al. 2009) were described as having bifid interlabia. In the current study, the bifid appearance of interlabia (Fig. 5c) was confirmed in light microscopy as well as in several SEM micrographs that clearly show this feature in both lateral and apical views of prepared specimens.

In multivariate analysis of eight measurements of *C. micropapillatum* and *C. bancrofti* in the present and other studies, the two species were poorly separated (Table 2; Fig. 7). In an ANOSIM test, morphometric variation between sexes and species was statistically significant, although modest in magnitude between sexes within the two species ($R=0.24$, $P=0.019$) and negligible between same-sex individuals of the two species ($R=0.025$, $P=0.017$). These results were essentially the same if data from Hartwich (1964), who included data from non-Australian sources of *C.* "*bancrofti*," were excluded from MDS (not shown) or ANOSIM (sex $R=0.253$, $P=0.017$, species $R=0.034$, $P=0.01$).

Contracaecum gibsoni Mattiucci et al. 2010

Synonyms: *Contracaecum multipapillatum* sp. A of Nascetti et al. (1990)

Site in host: Ventriculus.

Representative DNA sequences: ON723780-87 (ITS rDNA), ON736833-37 (*cox*2 mtDNA);

Adult stage: Body stout. Cuticle transversally striated. Dorsal and ventro-lateral lips with slight medial depression on upper margin (Figs. 8a–c and 9a–b); dorsal lip with 2 double papillae; each ventro-lateral lip with 1 double papilla, 1 single papilla, and 1 amphid. Interlabia triangular, wider at base, with rounded non-bifurcate tip (Figs. 8b and 9a). Excretory pore at base of lips. Esophagus with globular ventriculus. Ventriculus with posterior appendix. Intestinal caecum three to four times longer than ventricular appendix.

Males ($n=4$): Total length 15.0–44.0 (27 ± 12.3). Nerve ring 0.35–0.41 (0.39 ± 0.035) from anterior end. Esophagus 2.95–6.65 (4.89) long. Ventricular appendix 0.53–0.70 (0.70) long. Intestinal caecum 2.10–2.28 (2.50) long;

Table 2 Comparative metrical data of males and females of *C. micropapillatum* and *C. bancrofti* from present research and past studies

	C. micropapillatum present study ($n=50$)	*C. bancrofti* present study ($n=2$)	*C. bancrofti* Shamsi et al., 2009 ($n=25$)	*C. bancrofti* Norman, 2005 ($n=6$)	*C. micropapillatum* Hartwich, 1964 ($n=10$)	*C. micropapillatum* Johnston and Mawson, 1941 ($n=$n.r)	*C. micropapillatum* Cram, 1927 ($n=$n.r.)
Males							
Body length	17.2 (10–34.2)	17 (16–18)	27.3 (16.7–33.8)	28.9 (26.4–31.7)	10.30–25.20	24	15–20
Esophagus length	3.27 (2.01–4.56)	3.0 (2.9–3.0)	4.17 (3.00–5.90)	3.57 (3.05–3.95)	2.18–3.74	3.2	2.7
Esophagus/body length	19.7% (12.3–25.5%)	17.5% (16.5–18.4%)	16% (13–19%)	–	14–21%	16.6%	15%
Ventricular appendix	0.85 (0.47–1.15)	0.8 (0.805–0.806)	0.95 (0.68–1.30)	0.73 (0.6–0.92)	0.50–1.16	–	0.44
Ventricular appendix/esophagus	26.7% (17.8–42.1%)	2.71% (2.7–2.73%)	24% (14–33%)	–	23–42%	20%	16%
Intestinal cecum	2.5 (1.47–3.79)	2.2 (2.18–2.3)	2.82 (1.85–4.55)	2.36 (2.05–2.65)	1.58–2.69	–	2.1
Intestinal caecum/esophagus	75.8% (55.7–86.3%)	76.7% (73.4–79.9%)	69% (46–82%)	–	40–88%	62.5%	66.6–75%
Right spicule	2.45 (1.02–3.37)	2.3 (2.1–2.5)	2.73 (2.23–3.14)	2.70 (2.45–3.10)	1.29–3.53	2.2–2.8	5.1
Left spicule	2.40 (1.05–3.48)	2.27 (2.2–2.3)	2.74 (2.36–3.17)	2.62 (2.45–2.85)	1.21–3.46	2.2–2.8	5.1
Spicules/body length	14% (8.6–19%)	13.6% (12.1–15.1%)	7–15%	–	9–16%	11.1–14.2%	28.3%
Tail	0.28 (0.19–0.41)	0.23 (0.21–0.25)	0.24 (0.18–0.31)	0.20 (0.16–0.23)	0.21–0.32	0.18–0.2	0.17
Tail/body length	1.7% (1–3.2%)	1.39% (1.17–1.6%)	0.9% (0.7–1.3%)	–	1–2%	–	0.9%
Females							
Body length	18.8 (10–40.7)		30.4 (19.5–55.0)	34.1 (31.0–37.0)	11.80–30.80	30	20–30
Esophagus length	3.29 (1.67–5.69)		4.2 (3.2–5.6)	4.01 (3.65–4.30)	2.62–4.12	–	3.1
Esophagus/body length	18.7% (12–22.3%)		14% (9–18%)	–	12–19%	10–14.3%	13.5%
Ventricular appendix	0.81 (0.44–1.67)		1.05 (0.42–1.46)	0.72 (0.63–0.85)	0.67–1.54	–	0.5
Ventricular appendix/esophagus	25.2% (14.2–40.2%)		25% (11–34%)	–	21–39	25%	16.1%
Intestinal cecum	2.48 (1.34–4.87)		3.01 (2.21–4.71)	2.70 (2.40–3.10)	2.00–3.47	–	2
Intestinal cecum/esophagus	75.6% (62.7–89.1%)		72% (65–91%)	–	76–88%	66.6–81%	64.5%
Vulva to anterior end	6.68 (1.76–14.11)		11.3 (7.8–15.8)	13.2 (11.95–14.80)	6.00–10.30	–	5.75
Vulva/body length	32% (15–59%)		38% (19–48%)	–	30–50%	44%	25%
Tail	0.33 (0.17–0.54)		0.34 (0.16–0.46)	0.36 (0.32–0.40)	0.28–0.41	0.34	–
Tail/body length	1.94 (1.1–2.6)		1.2% (0.6–1.8%)	–	1–2%	–	–

n.r. not reported

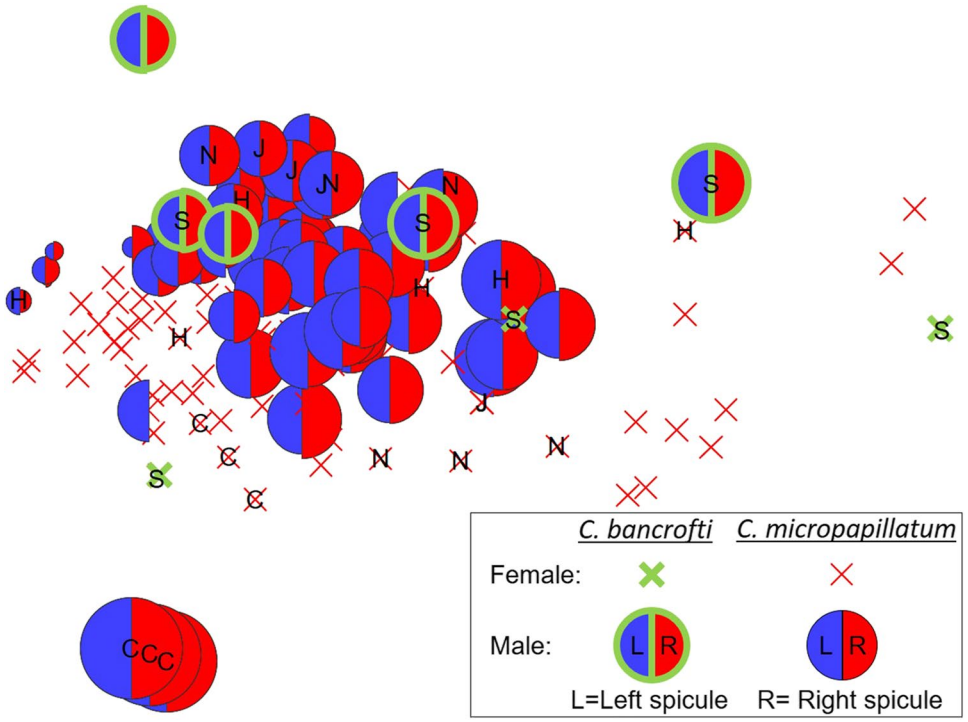

Fig. 7 Non-metric multidimensional scaling of eight morphometric distances in the present and other studies of *C. micropapillatum* (Stossich 1890) and *C. bancrofti* Johnston and Mawson 1941. Points are shape- and color-coded by worm sex and species (see inset legend) and labelled by source, with unlabelled points representing individual worms in the present study. Other studies are S = Shamsi et al. 2009; N = Norman (2005) cited in Shamsi et al. 2009; J = Johnston and Mawson 1941; C = Cram 1927; H = Hartwich 1964. Data point sizes for male worms are proportionate to spicule lengths (see inset legend). Two-dimensional stress = 0.16

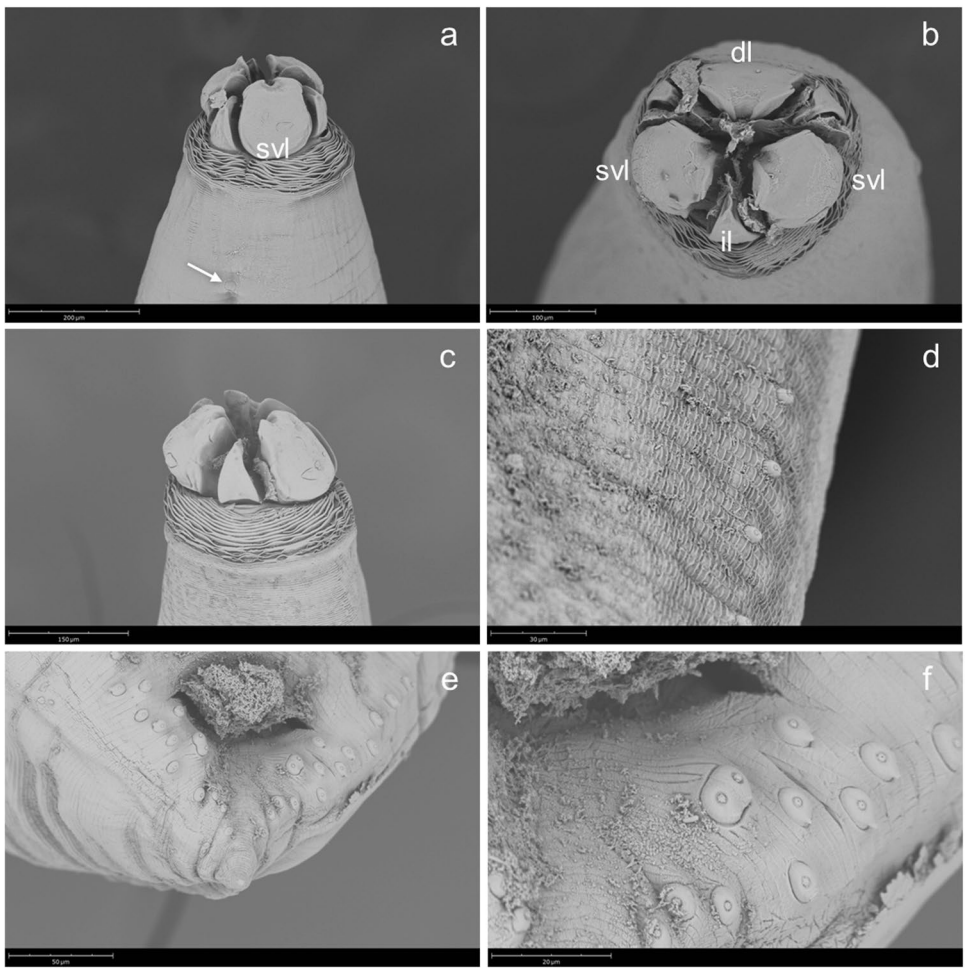

Fig. 8 SEM micrographs of *C. gibsoni* adult males: **a**) subventral view of anterior end showing the shape of subventral lip and the position of the amphid (arrow); **b**) apical view of anterior end showing dorsal lip (dl) with two ovoid papillae, subventral lips (svl) and simple non-bifurcated interlabium (il); **c**) detailed ventral view of anterior end; **d**) ventral view of caudal end showing precloacal papillae; **e**) ventral view of caudal end showing the characteristic pattern of paracloacal and post-cloacal papillae; **f**) detail of the pyriform-shaped proximal and paracloacal papillae

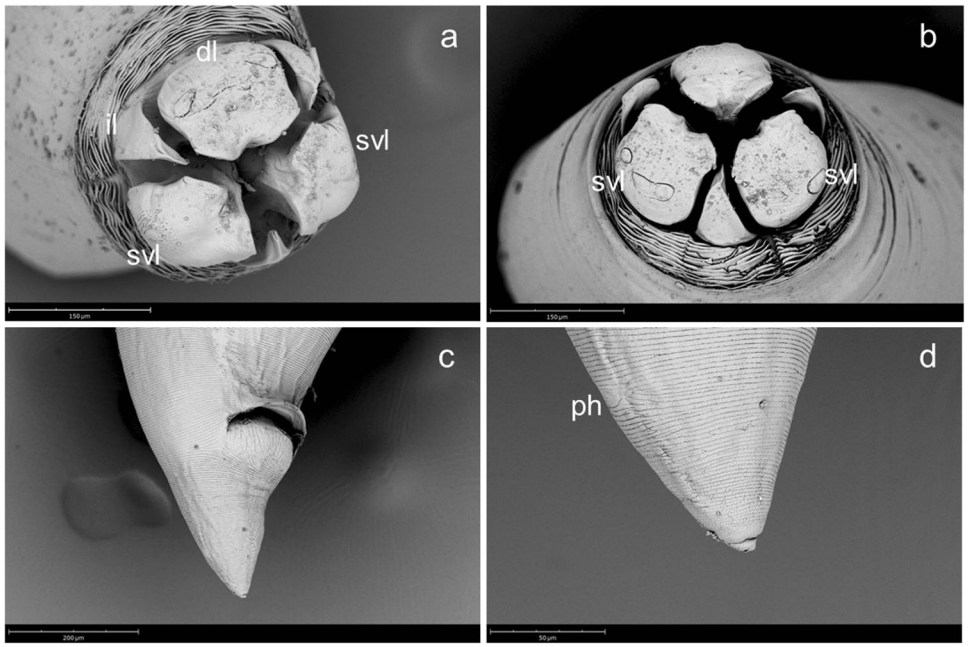

Fig. 9 SEM micrographs of *C. gibsoni* adult females: **a**) subapical view of anterior end showing dorsal lip (dl) with two ovoid papillae, subventral lips (svl) and simple non-bifurcated interlabium (il); **b**) subapical view of anterior end showing the shape of subventral lips; **c**) caudal end; **d**) detail of caudal tip, with phasmid (ph)

intestinal caecum/ventricular appendix length ratio 2.5–4.5 (3.8). Spicules slightly subequal; right spicule 1.82–2.50 (2.11 ± 0.29) long; left spicule 1.75–2.18 (1.99 ± 0.19) long; spicule tip pointed. Ratio spicules length/total length (spi/len) 0.04–0.12 (0.07). Precloacal papillae simple, forming 2 subventral lines (Fig. 8d). Five pairs of proximal papillae posterior to cloaca, lateral to paracloacal papillae, four of which pyriform in shape (Fig. 8e–f). Single pair of double paracloacal papillae; 4 pairs of distal papillae. Single pair of small papilla-like phasmids lateral to the distal pair (d4) of post-cloacal papillae (Fig. 8e). Tail 0.21–0.24 (0.23 ± 0.017) long.

Females ($n = 16$) Total length 13.0–63.0 (36.9 ± 14.5). Nerve ring 0.32–0.60 (0.49 ± 0.083) from anterior end. Esophagus 3.20–6.79 (5.10 ± 1.22) long. Ventricular appendix 0.85–1.42 (1.10 ± 0.16) long. Intestinal caecum 2.38–6.36 (4.31 ± 1.24) long, intestinal caecum/ventricular appendix length ratio 2.7–4.4 (3.8). Vulva in first third of body, 6.92–17.33 (12.90 ± 2.95) from anterior end. Tail conical, 0.21–0.60 (0.48 ± 0.09) long (Fig. 9c–d).

Remarks

Overall, measurements of our male and female specimens overlap data reported by Mattiucci et al. (2010), although our samples include also smaller and larger specimens. With respect to male features, the average ratio spi/len, spicule shape, and pattern of caudal papillae are the same as those reported in the original description of *C. gibsoni* (Mattiucci et al. 2010); such features have been considered as useful taxonomic criteria for distinguishing genetically detected sibling species of *Contracaecum* (Mattiucci et al. 2010). Particularly, as suggested by Shamsi and colleagues (2008), the arrangement and shape of the caudal papillae of males could be useful to differentiate cryptic species of the *C. multipapillatum* complex. In addition to its original description, the present work adds further morphological material providing the first SEM images of *C. gibsoni* male and female adults. Particularly, SEM micrographs of the caudal region of male specimens showed the presence of five proximal pairs of single papillae of which four pyriform in shape (Fig. 8e), a feature here reported for the first time in *C. gibsoni*.

Contracaecum quadripapillatum Saad et al. 2018

Site in host: Stomach and esophagus.

Representative DNA sequences: ON714979-86 (ITS rDNA), ON736806-07 (*cox*2 mtDNA).

Adult stage: Body stout. Cuticle transversally striated. Dorsal and ventro-lateral lips with central depression on upper margin (Figs. 10a and 11a); dorsal lip with 2 ovate papillae; each ventro-lateral lip with 1 ovate papilla. Interlabia triangular, wider at base, with rounded non-bifurcate tip (Fig. 10b). Short cuticular collar, interrupted laterally at the base of lips. Intestinal caecum three to five times longer than ventricular appendix.

Males: ($n = 3$) Total length 21.0–42.4 (20.8 ± 21.2). Nerve ring 0.45–0.63 (0.54 ± 0.09) from anterior end. Esophagus 3.60–4.99 (4.29 ± 0.069) long. Ventricular appendix 0.60–0.83 (0.74 ± 0.12) long. Intestinal caecum 2.06–4.39 (3.22 ± 1.16) long; intestinal caecum/ventricular appendix length ratio 2.5–5.6 (4.5). Spicules subequal, with rounded, spoon-like, flattened tip (Fig. 10c–d). Right spicule 2.27–2.52 (2.39 ± 0.13) long, left spicule 1.87–2.72 (2.32 ± 0.42) long 11.2–11.5% of body length. Post-cloacal

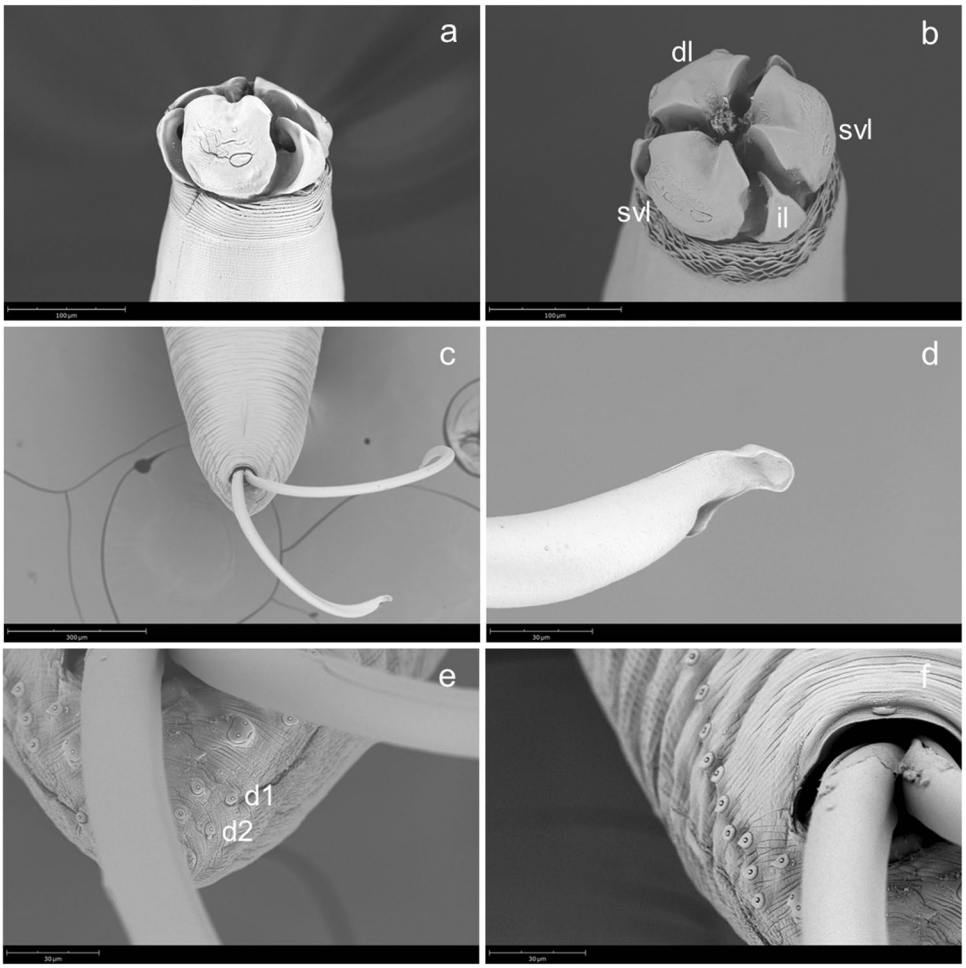

Fig. 10 SEM micrographs of *C. quadripapillatum* adult males: **a**) subventral view of anterior end showing the shape of the subventral lip with single ovoid papilla and short cuticular collar; **b**) apical view of anterior end showing dorsal lip (dl) with two ovoid papillae, subventral lips (svl) and simple non-bifurcated interlabium (il); **c**) ventral view of caudal end with everted spicule; **d**) detail of spicule tip; **e**) detail of the caudal end showing the characteristic pattern of caudal papillae, particularly, the first (d1) and second (d2) pair of distal papillae forming a square; **f**) detail of the caudal end showing pyriform-shaped paracloacal papillae

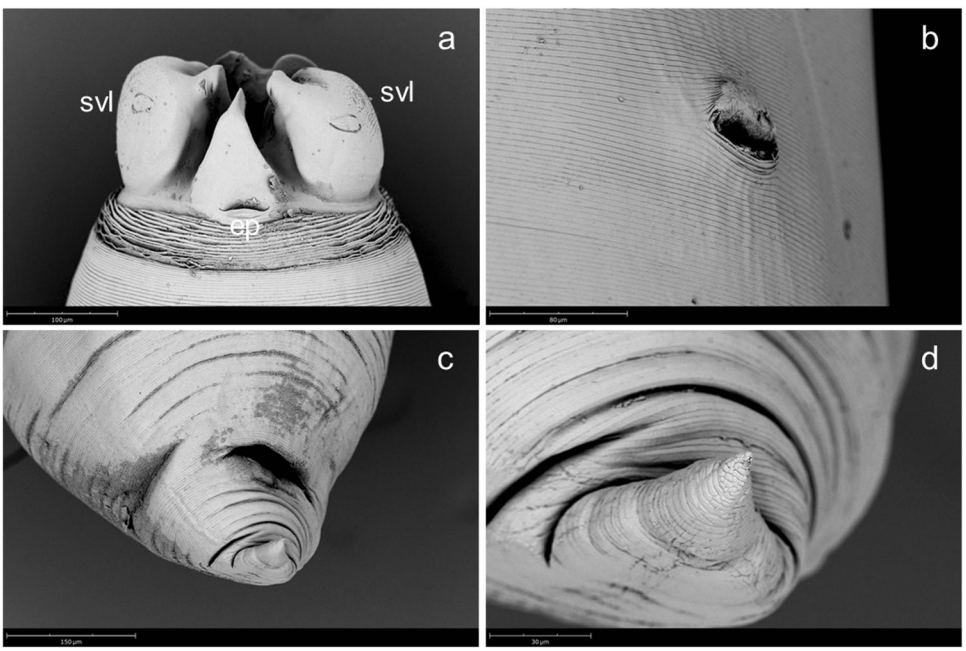

Fig. 11 SEM micrographs of *C. quadripapillatum* adult females: **a**) ventral view of anterior end, showing the excretory pore (ep) at the base of ventral interlabium, between subventral lips (svl); **b**) detail of the vulva; **c**) caudal end; **d**) detail of caudal tip

papillae consisting in two pairs of single papillae, followed by one pair of double papillae; remaining post-cloacal papillae arranged in three rows, first and second rows containing four papillae on each side forming quadrilateral shape, third row with one papilla on each side (Fig. 10e–f).

Females: ($n=4$) Total length 31.0–64.0 (40.5 ± 15.7). Nerve ring 0.33–0.56 (0.46 ± 0.10) from anterior end. Esophagus 4.73–5.65 (5.08 ± 0.44) long. Ventricular appendix 0.85–1.09 (0.95 ± 0.1) long. Intestinal caecum 3.95–4.46 (4.28 ± 0.32) long. Intestinal caecum/ventricular appendix length ratio 3.8–4.9 (4.5). Vulva in first third of body, 7.73–15.38 (10.48 ± 3.36) from anterior end (Fig. 11b). Tail conical, 0.38–0.47 (0.42 ± 50.5) long (Fig. 11c–d).

Remarks

Overall, measurements of male and female specimens of *C. quadripapillatum* reported by Saad and colleagues (2018) fall within a narrower range than our observations, possibly because Saad et al. (2018) measured experimentally obtained specimens belonging to exactly the same developmental stage, while specimens analyzed in the present study were recovered from naturally infected birds who likely acquired parasites in multiple feeding events. With respect to male morphological features of taxonomic value, the average ratio spi/len was slightly higher in our specimens (11% as compared to 8% reported by Saad et al. 2018), while spicule shape and pattern of caudal papillae are similar to those described by the latter authors. While the pyriform-shaped precloacal papillae in some cases (Fig. 10f) resemble *C. pyripapillatum*, the post-cloacal papillae of *C. quadripapillatum* form a square (Fig. 10e) and the tip of male's spicules is completely different (Fig. 10d) from *C. pyripapillatum*. In addition, the ITS rDNA of *C. pyripapillatum* is distant from *C. quadripapillatum* (Fig. 2).

Discussion

Prior to this study, in several valid species of *Contracaecum*, only either ITS rDNA or *cox*2 mtDNA were available, making comparison of sequences impossible. For example, only ITS was available in Australian *C. bancrofti*, while in *C. micropapillatum*, only *cox*2 and 28S rDNA had been sequenced. We resolved this problem by obtaining data from both markers in both species and avoided potential confusion from single-marker results (particularly ITS). While ITS sequences from Israeli and Australian isolates in the *C. bancrofti* + *C. micropapillatum* clade formed reciprocally monophyletic subclades, they had only moderate statistical support and were nearly identical (99.5% similarity). However, the *cox*2 of the specimens formed well-supported clades with unambiguous levels of sequence divergence, and gaps unique to *C. bancrofti* in the ITS alignment were not reflected in divergence calculations, or in phylogenetic analysis. We attempted to make further distinctions in sequenced specimens of these two species with both light microscopy and SEM, with particular attention to characters useful in distinguishing anisakids, such as interlabial structure, distribution pattern of male caudal papillae, spicule length and tip shape, size and pattern of caudal papillae (Fagerholm 1989; Mattiucci et al. 2010), as well as quantitative visualization of morphometric variation in *C. micropapillatum* and *C. bancrofti* in the present and past studies. Ultimately, while molecular evidence supports the validity of *C. bancrofti* as described by Shamsi et al. (2009), no morphological distinctions were observed that reliably separate this species from *C. micropapillatum*. Morphological variation in Table 2 and Fig. 7 may be inflated by variation in preservation methods among studies, or mixed-species infections undetected in non-molecular studies (i.e., those other than Shamsi et al. 2009 and the present work), but even stable characters such as spicule length are notably uninformative. In the future, sequences of *cox*2 from regional isolates of *C. micropapillatum* are needed to verify the wide geographic distribution and diverse host range that ITS-based and morphological records imply for this species, which has been reported from all the continents (China, Australia, Croatia, England, Congo, Mexico, USA), as well as in birds from several different families (Li et al. 2016), namely: Anseriformes (Anatidae): *Bucephala clangula* (L.); *Mergus squamatus* Gould; *Spatula clypeata* L.; Charadriiformes (Stercorariidae): *Stercorarius pomarinus* (Temminck); Pelecaniformes (Ardeidae): *Ardea alba* L.; *A. purpurea* L.; *Butorides striata* L., *B. striata atricapilla* (Afzelius); *Nyctanassa violacea* (L.); Pelecaniformes (Pelecanidae): *Pelecanus crispus* Bruch; *P. conspicillatus* Temminck; *P. erythrorhynchos* Gmelin; *P. onocrotalus* L.; *P. rufescens* Gmelin; *Pelecanus* sp.; Pelecaniformes (Phalacrocoracidae): *Microcarbo africanus* (Gmelin); *M. pygmaeus* (Pallas); *Phalacrocorax brasilianus* (Gmelin); *P. africanus* (Gmelin); *P. carbo* (L.); *Phalacrocorax* sp.

Joint analysis of both nuclear and mitochondrial markers was also necessary to resolve conflicting ITS and *cox2* results from *C. gibsoni*. In five adults from Israel collected in the present study, *cox2* matched *C. gibsoni* (syn *C. multipapillatum* A of Nascetti et al. 1990) described from *P. crispus* in Greece (p-distance 0–0.1% to data from Mattiucci et al. 2010). Had we obtained only ITS sequences, however, these specimens of *C. gibsoni* could have been mis-identified within the already-complicated *C. multipapillatum* complex, because the ITS matched data from specimens identified as *C. multipapillatum* (syn *C. multipapillatum* A of Nascetti et al. 1990). In addition to the *cox2* results, morphological features of these specimens overlapped with *C. gibsoni* as described by Mattiucci et al. (2010) and were supported

with SEM micrographs of adult male and female structures, to better characterize features poorly visible by light microscopy.

Contracaecum gibsoni was described from the Dalmatian pelican *P. crispus* L. (Pelecaniformes: Pelecanidae) from Greece and is now reported for the first time in *P. onocrotalus* L. from Israel. According to Mattiucci et al. (2010), species in the *C. multipapillatum* complex are restricted to the families Pelicanidae and Ardeidae from Central and South America, but in the Mediterranean areas they have been found only in pelicans, as demonstrated for *C. gibsoni* and *C. overstreeti*.

The adults of *C. quadripapillatum* were first described by Saad et al. (2018) after experimental infection of *P. erythrorhynchos* fed *Clarias lazera* from Lake Nasser, South Egypt naturally infected with L3s. These authors also obtained ITS rDNA sequences from *C. quadripapillatum* to which our specimens are identical (p-distance 0%). We here provide a new PCR–RFLP (*Ssp*I) assay to distinguish *C. quadripapillatum* from *C. gibsoni*, which are not resolved by the *Msp*I enzyme of Zhu et al. (2007), as well as *cox*2 mtDNA from both species, and new records in *P. onocrotalus* sampled in Israel.

The status and distributions of species of *Contracaecum* encountered here should be considered alongside the habits and movements of their definitive host, the great white pelican *P. onocrotalus*, one of the largest members of the family Pelecanidae. Populations of this gregarious bird are distributed in eastern Europe, Asia, and Africa. However, great white pelicans are not found in Australia, which is inhabited by *P. conspicillatus*. The disjunct distributions of the definitive hosts (*P. onocrotalus*, *P. conspicillatus*) are of interest given the apparent sister relationship and lack of morphological distinctions between their parasites, *C. bancrofti* and *C. micropapillatum*. Interestingly, phylogenetic analysis indicates *P. onocrotalus* is a basal, sister lineage to an Old-World clade of pelicans that includes *P. conspicillatus* (Kennedy et al. 2013).

Crivelli and Schreiber (1984) distinguished two geographically separate populations of the great white pelican: one in Africa and the other in eastern Europe and Asia. The African population is sedentary, living under tropical climatic conditions and the Eurasian population is migratory, visiting the Palearctic in spring and summer, during the breeding season (Crivelli et al. 1991). A few hundred of the migratory *P. onocrotalus* regularly winter in Israel, where they arrive from July to September, while thousands of individuals continue their migration to winter either in Sudan or in eastern central Africa (e.g., Ethiopia, Kenya, Uganda, Tanzania, or Zaïre). Several wintering grounds are also known in western and southern Asia, in Russia, Iran, Iraq, Pakistan, and India (Scott and Carp 1982; Van der Ven 1987, 1988; Crivelli et al. 1991). The same wetlands are used as stopovers, both in spring and autumn. Crivelli and colleagues (1991) reported that Great White Pelicans do not feed systematically at each stopover, either because the wetlands visited do not provide favorable feeding conditions or because the fish density is too low, or because the costs in time and energy would be too great. The fish ponds situated in northern Israel provide a favorable feeding environment being extremely rich in fish (Sarig 1990) and are subject to intensive foraging by migrating pelicans (Crivelli et al. 1991). In contrast, the Mediterranean Sea is rarely used as a feeding site by Great White Pelicans, which is consistent with the lack of recovered *Contracaecum* species that are distributed in brackish or saltwater environments (e.g., *Contracaecum rudolphii* A). In addition, the numerical dominance of *C. micropapillatum* compared to the other species encountered, as revealed by RFLP analysis, is consistent with its putatively wide geographic distribution (Poulin 2007), which extends beyond the range of *P. onocrotalus* to the Americas. The relative abundance of *C. micropapillatum* is also consistent with the general frequency with which this species is reported (Shamsi et al. 2009, 2019).

Taken together, our results provide further illustration that more than one marker (preferably independent, e.g., one nuclear, one mitochondrial) provide better support for distinguishing helminths characterized by genetic variability and lacking clear morphological differences, such as those within the *Anisakis simplex*, *Pseudoterranova decipiens*, and *Contracaecum multipapillatum* complexes (Nadler and Hudspeth 2000; Paggi et al. 2000; Mattiucci et al. 2005) and other anisakids (Valentini et al. 2006; Mattiucci et al. 2008, 2010, 2020; D'Amelio et al. 2020).

Such data should be generated in any study focused on the genetic diversity of this group of parasites, to help clarifying not only their taxonomy but also possible cospeciation patterns between *Contracaecum* spp. and different families of their definitive hosts, as already suggested for other anisakid taxa (Mattiucci and Nascetti 2006, 2008).

Acknowledgements The authors are grateful for the constructive comments of anonymous reviewers on early versions of this manuscript, and express particular thanks to the editor dr. Shokoofeh Shamsi, who kindly provided specimens of *C. bancrofti* from Australia.

Author contribution MC and PT wrote the main manuscript text, carried out the analyses, and prepared all the figures. MN and MN provided the technical support for SEM and molecular analyses. ND and RK carried out the sampling and necropsies. SL carried out the multivariate analysis and revised the manuscript. AG and MLF revised the manuscript. All authors reviewed the manuscript and approved the final manuscript.

Funding This study was supported by the Israeli Veterinary Services and by the University of Bologna, Italy. Scanning Electron Microscopy acquired thanks to the Department of Excellence Project 2018–2022 funded by the Italian Ministry of Education, Universities and Research. SAL was supported by the National Science Foundation (DEB award 1845021).

Data availability The DNA sequences generated in this study have been deposited on the public database GenBank.

Declarations

Ethical approval "Not applicable".

Consent to participate "Not applicable".

Consent for publication "Not applicable".

Conflict of interest The authors declare no competing interests.

References

Anderson RC (2000) Nematode parasites of vertebrates: their development and transmission, 2nd edn. CABI, Wallingford

Ángeles-Hernández JC, Gómez-de Anda FR, Reyes-Rodríguez NE, Vega-Sánchez V, García-Reyna PB, Campos-Montiel RG, Calderón-Apodaca NL, Salgado-Miranda C, Zepeda-Velázquez AP (2020) Genera and species of the Anisakidae family and their geographical distribution. Animals 10:2374. https://doi.org/10.3390/ani10122374

Baruš V, Sergeeva TP, Sonin MD, Ryzhikov KM (1978) Helminths of fish-eating birds of the Palaearctic Region: Nematoda. In: Rysavy B, Ryzhikov KM (eds) Helminths of fish-eating birds. Springer, Praha, p 318

Blouin MS (2002) Molecular prospecting for cryptic species of nematodes: mitochondrial DNA versus internal transcribed spacer. Int J Parasitol 32:527–531. https://doi.org/10.1016/s0020-7519(01)00357-5

Cram EB (1927) Bird parasites of the nematode suborders Strongylata, Ascaridata, and Spirurata. Bull US Natl Mus 492. https://doi.org/10.5479/si.03629236.140.1

Crivelli AJ, Schreiber RW (1984) Status of Pelecanidae. Biol Conserv 30:147–156

Crivelli AJ, Leshem Y, Mitchev T, Jerrentrup H (1991) Where do palearctic great white pelicans (*Pelecanus onocrotalus*) presently overwinter? Rev Ecol-Terre Vie 46:145–171

D'Amelio S, Lombardo F, Pizzarelli A, Bellini I, Cavallero S (2020) Advances in omic studies drive discoveries in the biology of *Anisakid* nematodes. Genes 11:801. https://doi.org/10.3390/genes11070801

Davidovich N, Tedesco P, Caffara M, Yasur-Landau D, Gustinelli A, Drabkin V, Minkova E, Aflalo O, Morick D, Fioravanti ML (2022) Morphological description and molecular characterization of *Contracaecum* larvae (Nematoda: Anisakidae) parasitizing market-size hybrid tilapia (*Oreochromis aureus* x *Oreochromis niloticus*) and red drum (*Sciaenops ocellatus*) farmed in Israel. Food Waterborne Parasitol 26:e00147. https://doi.org/10.1016/j.fawpar.2022.e00147

Fagerholm HP (1989) Intra-specific variability of the morphology in a single population of the seal parasite *Contracaecum osculatum* (Rudolphi) (Nematoda: Ascaridoidea), with a redescription of the species. Zool Scr 18:33–41. https://doi.org/10.1111/j.1463-6409.1989.tb00121.x

Fagerholm HP, Overstreet RM (2008) Ascaridoid Nematodes: *Contracaecum*, *Porrocaecum*, and *Baylisascaris*. In: Atkinson CT, Thomas NJ, Hunter DB (eds) Parasitic diseases of wild birds. Wiley-Blackwell, Iowa, USA, pp 413–433. https://doi.org/10.1002/9780813804620.ch24

Hall TA (1999) BioEdit: A user-friendly biological sequence alignment editor and analysis program for Windows 95/98/NT. Nucleic Acids Symp Ser 41:95–98

Hamouda AH, Younis AE (2022) Molecular characterization of zoonotic anisakid *Contracaecum* spp. larvae in some fish species from Lake Nasser. Egypt Aquac Res 53:2548–2561. https://doi.org/10.1111/are.15774

Hartwich G (1964) Revision der vogelparasitischen nematoden Mitteleuropas II. Die gattung *Contracaecum* Railliet and Henry, 1912 (Ascaridoidea). Mitt Zool Mus Berl 40:15–53

Johnston TH, Mawson PM (1941) Ascaroid nematodes from Australian birds. Trans R Soc S Aust 65:110–115

Kennedy M, Taylor SA, Nádvorník P, Spencer HG (2013) The phylogenetic relationships of the extant pelicans inferred from DNA sequence data. Mol Phyl Evol 66:215–222. https://doi.org/10.1016/j.ympev.2012.09.034

Kumar S, Stecher G, Tamura K (2016) MEGA7: Molecular Evolutionary Genetics Analysis version 7 for bigger datasets. Mol Biol Evol 33:1870–1874. https://doi.org/10.1093/molbev/msw054

Kumar S, Periyasamy A, Rao NVR, Sunil SS, Kumara HN, Sundararaj P, Chidananda G, Sathish A (2019) Multiple infestations of gastrointestinal parasites—probable cause for high mortality of Spot-billed Pelican (*Pelecanus philippensis*) at Kokrebellur Community Reserve, India. Int J Parasitol Parasites Wildl 9:68–73. https://doi.org/10.1016/j.ijppaw.2019.04.001

Li L, Gibson DI, Zhang LP (2016) An annotated catalogue of the ascaridoid nematode parasites of Chinese vertebrates. Syst Parasitol 93:1–35. https://doi.org/10.1007/s11230-015-9617-5

Mattiucci S, Nascetti G (2006) Molecular systematics, phylogeny and ecology of anisakid nematodes of the genus *Anisakis* Dujardin, 1845: an update. Parasite 13(2):99–113. https://doi.org/10.1051/parasite/2006132099

Mattiucci S, Nascetti G, Dailey M, Webb SC, Barros N, Cianchi R, Bullini L (2005) Evidence for a new species of *Anisakis* Dujardin, 1845: Morphological description and genetic relationships between congeners (Nematoda: Anisakidae). Syst Parasitol 61:157–171. https://doi.org/10.1007/s11230-005-3158-2

Mattiucci S, Nascetti G (2008) Advances and trends in the molecular systematics of anisakid nematodes, with implications for their evolutionary ecology and host parasite co-evolutionary processes. Adv Parasitol 66:47–148. https://doi.org/10.1016/S0065-308X(08)00202-9

Mattiucci S, Paoletti M, Webb SC, Sardella N, Timi JT, Berland B, Nascetti G (2008) Genetic relationships among species of *Contracaecum* Railliet & Henry, 1912 and *Phocascaris* Host, 1932 (Nematoda: Anisakidae) from pinnipeds based on mitochondrial cox2 sequences, and congruence with allozyme data. Parasite 15:408–419. https://doi.org/10.1051/parasite/2008153408

Mattiucci S, Paoletti M, Solorzano AC, Nascetti G (2010) *Contracaecum gibsoni* n. sp. and *C. overstreeti* n. sp. (Nematoda: Anisakidae) from the dalmatian pelican *Pelecanus crispus* (L.) in Greek waters: genetic and morphological evidence. Syst Parasitol 75:207–224. https://doi.org/10.1007/s11230-009-9220-8

Mattiucci S, Sbaraglia GL, Palomba M, Filippi S, Paoletti M, Cipriani P, Nascetti G (2020) Genetic identification and insights into the ecology of *Contracaecum rudolphii* A and *C. rudolphii* B (Nematoda: Anisakidae) from cormorants and fish of aquatic ecosystems of Central Italy. Parasitol Res 119:1243–1257. https://doi.org/10.1007/s00436-020-06658-8

McDaniel B, Patterson I (1966) Nematode infestation of a white pelican found along the gulf coast of Texas. Southwest Nat 11:312–312

Nadler SA, Hudspeth DSS (2000) Phylogeny of the Ascaridoidea (Nematoda: Ascaridida) based on three genes and morphology: hypotheses of structural and sequence evolution. J Parasitol

86:380–393. https://doi.org/10.1645/0022-3395(2000)086[0380:POTANA]2.0.CO;2
Nascetti G, Bullini L, Cianchi R, Paggi L, Orecchia P, Mattiucci S, D'Amelio S, Berland B (1990) Genetic relationships among anisakid species belonging to the genera *Contracaecum* and *Phocascaris*. Bull Soc Fr Parasitol 8:261
Otachi EO, Szostakowska B, Jirsa F, Fellner-Frank C (2014) Parasite communities of the elongate tigerfish *Hydrocynus forskahlii* (Cuvier 1819) and redbelly tilapia *Tilapia zillii* (Gervais 1848) from Lake Turkana, Kenya: influence of host sex and size. Acta Parasitol 60:9–20. https://doi.org/10.1515/ap-2015-0002
Paggi L, Mattiucci S, Gibson DI, Berland B, Nascetti G, Cianchi R, Bullini L (2000) *Pseudoterranova decipiens* species A and B (Nematoda: Ascaridoidea): Nomenclatural designation, morphological diagnostic characters and genetic markers. Syst Parasitol 45:185–197. https://doi.org/10.1023/a:1006296316222
Poulin R (2007) Are there general laws in parasite ecology? Parasitology 134:763–776. https://doi.org/10.1017/S0031182006002150
Pronkina NV, Spiridonov SE (2018) Morphological and molecular characterization of anisakid juveniles from the golden grey mullet of the Black Sea. Russ J Nematol 26:87–92. https://doi.org/10.24411/0869-6918-2018-10008
Rokicki J, Sołtysiak Z, Dziekońska-Rynko J, Borucińska J (2011) Pathology associated with *Contracaecum rudolphii* (Nematoda: Anisakidae) infection in the great cormorant *Phalacrocorax carbo* (L. 1758). Helminthol 48:28–35. https://doi.org/10.2478/s11687-011-0006-6
Saad AI, Younis AE, Rabei JM (2018) Experimental life cycle of *Contracaecum quadripapillatum* n. sp. in white pelican (*Pelecanus erythrorhynchos*) at Lake Nasser, Egypt: morphological and genetic evidences. J Egypt Soc Parasitol 48:587–598
Sarig S (1990) The fish culture industry in Israel in 1989. lsraeli J Aquacult Bamidgeh 42:39–45
Scott DA, Carp E (1982) A midwinter survey of wetlands in Mesopotamia, Iraq, 1979. Sandgrouse 4:60–76
Shamsi S, Aghazadeh-Meshgi M (2011) Morphological and genetic characterisation of selected *Contracaecum* (Nematoda: Anisakidae) larvae in Iran. Iran J Fish Sci 10:356–361
Shamsi S, Gasser R, Beveridge I, Shabani AA (2008) *Contracaecum pyripapillatum* n. sp. (Nematoda: Anisakidae) and a description of *C. multipapillatum* (von Drasche, 1882) from the Australian pelican *Pelecanus Conspicillatus*. Parasitol Res 103:1031–1039. https://doi.org/10.1007/s00436-008-1088-z
Shamsi S, Norman R, Gasser R, Beveridge I (2009) Redescription and genetic characterization of selected *Contracaecum* spp. (Nematoda: Anisakidae) from various hosts in Australia. Parasitol Res 104:1507–1525. https://doi.org/10.1007/s00436-009-1357-5
Shamsi S, Steller E, Chen Y (2018) New and known zoonotic nematode larvae within selected fish species from Queensland waters in Australia. Int J Food Microbiol 272:73–82. https://doi.org/10.1016/j.ijfoodmicro.2018.03.007
Shamsi S, Turner A, Wassens S (2018) Description and genetic characterization of a new *Contracaecum* larval type (Nematoda: Anisakidae) from Australia. J Helminthol 92:216–222. https://doi.org/10.1017/S0022149X17000360
Shamsi S, Stoddart A, Smales L, Wassens S (2019) Occurrence of *Contracaecum bancrofti* larvae in fish in the Murray-Darling Basin. J Helminthol 93:574–579. https://doi.org/10.1017/S0022149X1800055X
Stossich M (1890) Elminti della Croazia. Glasnik Hrvatskoga Naravoslovnoga Društva 5:129–136
Stossich M (1896) Il Genere *Ascaris* Linné. Lavoro monografico. Boll Soc Adriat Sci Nat Trieste 17:9–114
Thabit A, Abdallah ESH (2022) Morphological and molecular identification of third-stage *Contracaecum* larvae (Nematoda: Anisakidae) parasitizing Nile perch *Lates niloticus* in Egypt. Aquac Res 53:4869–4881. https://doi.org/10.1111/are.15980
Valentini A, Mattiucci S, Bondanelli P, Webb SC, Mignucci-Giannone AA, Colom-Llavina MM, Nascetti G (2006) Genetic relationships among *Anisakis* species (Nematoda: Anisakidae) inferred from mitochondrial *cox*2 sequences, and comparison with allozyme data. J Parasitol 92:156–166. https://doi.org/10.1645/GE-3504.1
Valles-Vega I, Molina-Fernández D, Benítez R, Hernández-Trujillo S, Adroher FJ (2017) Early development and life cycle of *Contracaecum multipapillatum s.l.* from a brown pelican *Pelecanus occidentalis* in the Gulf of California, Mexico. Dis Aquat Org 125:167–178. https://doi.org/10.3354/dao03147
Van Der Ven J (1987) Asian waterfowl 1987. Midwinter bird observations in most Asian countries. IWB, Slimbridge, England
Van Der Ven J (1988) Asian waterfowl 1988. Midwinter bird observations in most Asian countries. IWRB, Slimbridge, England
Yamaguti S (1935) Studies on the helminth fauna of Japan. Part 12. Avian nematodes. I J J Zool 6:403–431
Yamaguti S (1961) Systema Helminthum. The Nematodes of Vertebrates. Part I. Interscience, New York, USA, 3:237–241
Zhu X, Gasser RB, Podolska M, Chilton NB (1998) Characterisation of anisakid nematodes with zoonotic potential by nuclear ribosomal DNA Sequences. Int J Parasitol 28:1911–1921. https://doi.org/10.1016/S0020-7519(98)00150-7
Zhu X, D'Amelio S, Paggi L, Gasser RB (2000) Assessing sequence variation in the internal transcribed spacers of ribosomal DNA within and among members of the *Contracaecum osculatum* complex (Nematoda: Ascaridoidea: Anisakidae). Parasitol Res 86:677–683. https://doi.org/10.1007/pl00008551
Zhu XQ, D'Amelio S, Gasser RB, Yang TB, Paggi L, He F, Lin RQ, Song HQ, Ai L, Li AX (2007) Practical PCR tools for the delineation of *Contracaecum rudolphii* A and *Contracaecum rudolphii* B (Ascaridoidea: Anisakidae) using genetic markers in nuclear ribosomal DNA. Mol Cell Probes 21:97–102. https://doi.org/10.1016/j.mcp.2006.08.004